Inductive and Conjugative S→C Polarizations in "Trithiocarbenium Ions" $[C(SH)_3]^+$ and $[C(SH)_3]^{\bullet,2+}$. Potential Energy Surface Analysis, Electronic Structure Motif, and Spin Density Distribution

Rainer Glaser,*,†,§ Godwin Sik-Cheung Choy,† Grace Shiahuy Chen,† and Hansjörg Grützmacher*,‡

Contribution from the Department of Chemistry, University of Missouri−Columbia, Columbia, Missouri 65211, and Institut für Anorganische Chemie, Eidgenössische Technische Hochschule, CH-8092 Zürich, Switzerland

Received March 22, 1996. Revised Manuscript Received July 9, 1996[⊗]

Abstract: The formation of $[C(SH)_3]^+$ (**a**) by hydride abstraction from $HC(SH)_3$ and its oxidation to the radical dication $[C(SH)_3]^{\bullet,2+}$ (**b**) were studied to examine the potential of stabilizing carbenium ions via trithio substitution. Potential energy surfaces (PES) were explored at the HF/6-31G* level and energies were refined at the (P)MP4-(full,sdtq)/6-31G* level without and with annihilation of spin contaminations. The unpaired π-electron in the radical lies well below the Fermi level and spin polarization and dynamic electron correlation become important. Open Y-conjugated structures **1** (C_{3h} or C_s) and their rotamers **2** (C_s) are favored. Four cyclic, S−S connected, distonic, chiral stereoisomers **3b** are local minima for the radical dication. The C−S rotational barriers to isomerization via **4** and automerization via **5** (two isomeric TSs) and the high energies of C_{3v} models **6** indicate stronger S−C π-interactions in the cations **1** and **2** than in the dications. C_{3h}-**1b** undergoes a Jahn−Teller distortion to C_s-**1b′** but pseudorotation is facile. The PES analyses suggest two strategies to achieve pyramidalization of the trivalent carbon in heteroatom-substituted carbenium ions via X−X interactions in CX_3^{n+} or via face-preferential hyperconjugation. The basic approach was found to be successful: The computed hydride affinity of **1a** is $\Delta HA = 95.5$ kcal/mol lower than for CH_3^+. ΔHA was partitioned into a methane destabilization of 32.0 kcal/mol and a carbenium ion stabilization of 63.5 kcal/mol. Our best estimate for the ionization energy of **1a** is IP(**1a**) = 343.8 kcal/mol (14.9 eV) and results in ΔH_f(**1b**) = 541.5 kcal/mol. The cations $[C(SH)_3]^+$ and $[C(SH)_3]^{\bullet,2+}$ show the same unexpected electronic motif. Strong S→C donations occur in the π- and σ-systems and, instead of charge dispersal, large positive SH charges are arranged around a *negative* C center. The stabilization mechanisms in the S-containing ions and the lighter O homologues are fundamentally different due to the *umpolung* of the C−X bonds. Oxidation of $[C(SH)_3]^+$ removes S-π-electron density and increases the π-acidity of the C atom. The α-spin density is concentrated on the S atoms and carbon is β-spin polarized.

Introduction

Oxidation generally leads to molecular distortions[1,2] and these are especially large when the HOMO of the non-oxidized molecule is strongly bonding or antibonding. Prominent examples include the pairs CH_4 (T_d) and CH_4^{2+} (planar, C_{2v})[3−5] as well as $C_6(CH_3)_6$ (planar) and $C_6(CH_3)_6^{2+}$ (pentagonal pyramid).[6] To observe the structural effects of twofold oxidation, several donors may be required to achieve sufficient stabilization of the highly charged species as is exemplified by the diamino derivative $(Me_2N)_2CC(NMe_2)_2^{2+}$ of $[H_2C-CH_2]^{2+}$.[7,8] We are interested in the stabilizing effects of third or higher row elements on carbenium ions.[9] In these compounds both σ- and π-donating effects account for stabilization. We have been studying the electronic properties of P analogs[10] **I** and **II** of diazonium ions[11] and we succeeded in the preparation of methylenephosphonium ions[12] **III** with different C substituents.

* Authors to whom correspondence should be addressed. R.G.: FAX (573) 882-2754, e-mail chemrg@showme.missouri.edu. H.G.: FAX (1) 6 32 10 90, e-mail gruetz@elwood.ethz.ch.

† University of Missouri−Columbia.

‡ ETH Zürich.

§ Presented in part in the Division of *Computers in Chemistry* at the 208th National ACS Meeting, Washington, DC, August 1994.

⊗ Abstract published in *Advance ACS Abstracts,* November 1, 1996.

(1) For elusive reviews see: (a) Bock, H.; Ruppert, K.; Näther, C.; Havlas, Z.; Herrmann, H. F.; Arad, C.; Göbel, I.; John, A.; Meuret, J.; Nick, S.; Rauschenbach, A.; Seitz, W.; Vaupel, T.; Solouki, B. *Angew. Chem., Int. Ed. Engl.* **1992**, *31*, 550 and literature cited therein. (b) Lammertsma, K.; Schleyer, P. v. R.; Schwarz, H. *Angew. Chem., Int. Ed. Engl.* **1989**, *28*, 1321.

(2) (a) Schastnev, P. V.; Shchegoleva, L. N. *Molecular Distortions in Ionic and Excited States*; CRC Press: New York, 1995. (b) See Chapter 4 in (a) and references cited therein.

(3) (a) Rabrenovic, M.; Proctor, C. J.; Ast, T.; Herbert, C. G.; Brenton, A. G.; Beynon, J. H. *J. Phys. Chem.* **1983**, *87*, 3305. (b) Stahl, D.; Maquin, F.; Gaumann, T.; Schwarz, H.; Carrupt, P.-A.; Vogel, P. *J. Am. Chem. Soc.* **1985**, *107*, 5049.

(4) Wong, M. W.; Radom, L. *J. Am. Chem. Soc.* **1989**, *111*, 1155.

(5) For the oxidation of ethylene, see: (a) Balaban, A. T.; de Mar'e, G. R.; Poisier, R. A. *J. Mol. Struct.* **1989**, *183*, 103. (b) Lammertsma, K.; Barzaghi, M.; Olah, G. A.; Pople, J. A.; Kos, A. J.; Schleyer, P. v. R. *J. Am. Chem. Soc.* **1983**, *105*, 5252.

(6) Hogeveen, H.; Kwant, P. W. *Acc. Chem. Res.* **1975**, *8*, 413.

(7) (a) Bock, H.; Ruppert, K.; Merzweiler, K.; Fenske, D.; Goesmann, H. *Angew. Chem., Int. Ed. Engl.* **1989**, *28*, 1684. (b) Ohwada, T.; Yamazaki, T.; Suzuki, T.; Saito, S.; Shudo, K. *J. Am. Chem. Soc.* **1996**, *118*, 6220.

(8) Comparable distortions were observed in the cations of [hexaazaoctahydrocoronene]$^{n+}$ ($n = 0-4$) which may be formally regarded as a hexaamino-substituted benzene: Miller, J. S.; Dixon, D. A.; Calabrese, J. C.; Vazquez, C.; Krusic, P. J.; Ward, M. D.; Wassermann, E.; Harlow, R. L. *J. Am. Chem. Soc.* **1990**, *112*, 381.

(9) (a) Apeloig, A.; Schleyer, P. v. R.; Pople, J. A. *J. Am. Chem. Soc.* **1977**, *99*, 1291. (b) Bernardi, F.; Mangini, A.; Epiotis, N. D.; Larson, J. R.; Shaik, S. *J. Am. Chem. Soc.* **1977**, *99*, 7465.

(10) (a) Glaser, R.; Horan, C. J.; Choy, G. S.-C.; Harris, B. L. *J. Phys. Chem.* **1992**, *96*, 3689. (b) Glaser, R.; Horan, C. J.; Haney, P. E. *J. Phys. Chem.* **1993**, *97*, 1835. (c) Phenyl systems: Glaser, R.; Horan, C. J., in preparation.

S0002-7863(96)00944-4 CCC: $12.00

Scheme 1

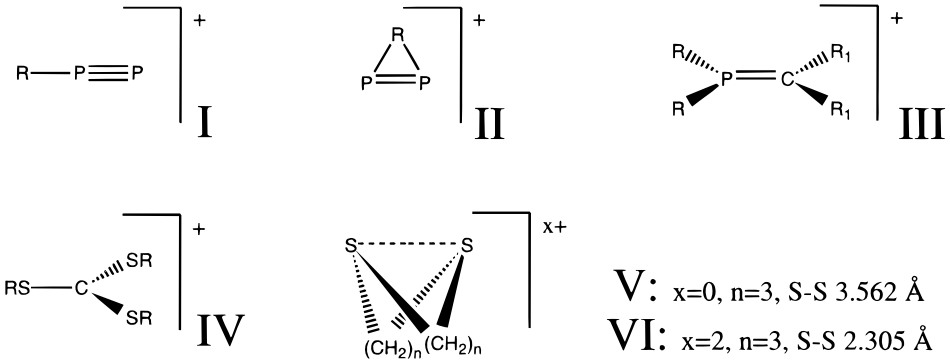

While diazonium ions may be considered as N_2 complexes of R^+,[13] the P analogs are completely different in that the P_2 group does carry the positive charge. Similarly and in contrast to iminium ions $R_2N{=}CR_2^+$, the trigonal planar coordinated P center bears a considerable positive charge while the C atom is negatively charged (up to −0.7).

As with phosphorus, sulfur is an attractive candidate to stabilize polycations[14] due to its low ionization potential and electronegativity.[15] Related to methylenephosphonium ions are the thiocarbenium ions **IV**.[16] Gompper and Kutter[17] described the preparation of $[(MeS)_3C]^+$ by alkylation of $(CH_3S)_2C{=}S$.[18] Olah et al. spectroscopically characterized cations of the types $[C(OH)_n(SH)_{3-n}]^+$ ($n = 0-3$) and trisubstituted carbenium ions with X = OH, SH, and NH_2 also were discussed.[19] The recent discovery that guandinium ions $(R_2N)_3C^+$ may play a crucial role in the catalytic activity of a metal free hydrogenase has renewed the interest in these systems.[20] X-ray crystal structures of several dithio-[21] and trithio-substituted[22] carbenium ions were obtained. More recently, evidence was provided for the existence of trithio-substituted silylenium ions[23] and several types of $[S(SX)_3]^+$ ions[24] were described (X = H, Cl). There is gas-phase evidence to suggest that S can stabilize carbenium ions better than does oxygen.[25] The stabilization of carbenium ions by adjacent heteroatoms has been discussed for monosubstituted systems[26,27] and there also have been some studies on the effects of multiple substitution.[28] Recently we could show experimentally and by ab initio calculations (MP2/LANL1DZ+P) that the different mechanism of stabilization can be brought to the fore only through consideration of multiple substitution in $[CH_n(XR)_{3-n}]^+$ (X = O, S, Se, Te; R(exp) = 2,4,6-i$Pr_3C_6H_2$, R(calc) = H; $n = 0-2$).[29] According to our evaluations of ΔH for the isodesmic reaction $[CH_n(XH)_{3-n}]^+ + nCH_4 \rightarrow nCH_3(XH) + CH_3^+$, monosubstituted ions $[CH_2(XH)]^+$ are equally stable for all X while di- and trisubstituted ions $[CH(XH)_2]^+$ and $[C(XH)_3]^+$ are considerably more stable for X = O than for the heavier homologs (X = S, Se, Te). A particularly noteworthy result of these theoretical studies concerns the discovery of enhanced charge separation in $[C(OH)_3]^+$ instead of the commonly expected charge delocalization. For this ion $[C(OH)_3]^+$, natural orbital population (NPA) suggested a positive charge on carbon (+1.3) that is larger than unity. The homologous ions $[C(XH)_3]^+$ (X = S, Se, Te) were found to differ greatly and indeed fundamentally in that the carbon center is negatively charged as the result of effective X→C donation in the σ- and π-systems. We will show below that the electronic features suggested by the NPA analysis are fully corroborated

(11) (a) Glaser, R.; Choy, G. S.-C. *J. Am. Chem. Soc.* **1993**, *115*, 2340. (b) Glaser, R.; Horan, C. J. *J. Org. Chem.* **1995**, *60*, 7518.

(12) (a) Heim, U.; Pritzkow, H.; Fleischer, U.; Grützmacher, H. *Angew. Chem., Int. Ed. Engl.* **1993**, *32*, 1359. (b) Heim, U.; Pritzkow, H.; Schoenberg, H.; Grützmacher, H. *J. Chem. Soc., Chem. Commun.* **1993**, 673. (c) Grützmacher, H.; Pritzkow, H. *Angew. Chem., Int. Ed. Engl.* **1992**, *31*, 99. (d) Grützmacher, H.; Pritzkow, H. *Angew. Chem., Int. Ed. Engl.* **1991**, *30*, 709.

(13) β,β-Disubstituted vinyldiazonium ions are best viewed as carbenium ions with an attached diazoalkyl group, e.g. $X_2C(+)\text{-}CRN_2$: (a) Chen, G. S.; Glaser, R.; Barnes, C. L. *J. Chem. Soc., Chem. Commun.* **1993**, 1530. (b) Glaser, R.; Chen, G. S.; Barnes, C. L. *Angew. Chem., Int. Ed. Engl.* **1992**, *31*, 740.

(14) Reviews: (a) Olah, G. A.; White, A. M. *Chem. Rev.* **1970**, *70*, 561. (b) Pittman, C. U., Jr.; McManus, S. P.; Larsen, J. W. *Chem. Rev.* **1972**, *72*, 357. (c) Sundaralingam, M.; Chwang, A. K. In *Carbonium Ions* ; Olah, G. A., Schleyer, P. v. R., Eds.; John Wiley & Sons, New York, 1976; Vol 5, pp 2427. (d) Olah, G. *Angew. Chem., Int. Ed. Engl.* **1993**, *32*, 767.

(15) Allen, L. C. *J. Am. Chem. Soc.* **1989**, *111*, 9003.

(16) See for example: (a) Okayama, T. In *Reviews on Heteroatom Chemistry;* Oae, S., Ed.; MYU: Tokyo, 1988, Vol. 1, p 46. (b) Claus, P. K. In *Methods of Organic Chemistry*; Houben-Weyl-Müller; Thieme Verlag: Stuttgart, Germany, 1985; p 1469. (c) Tucker, W. P.; Glenn, L. R. *Tetrahedron Lett.* **1967**, *29*, 2747. (d) Stahl, I.; Kuehn, I. *Chem. Ber.* **1983**, *116*, 1739. (e) Frasch, M.; Mono, S.; Pritzkow, H.; Sundermeyer, W. *Chem. Ber.* **1993**, *126*, 273.

(17) Gompper, R.; Kutter, E. *Chem. Ber.* **1965**, *98*, 1365.

(18) Tucker, W. P.; Roof, G. L. *Tetrahedron Lett.* **1967**, 2747.

(19) (a) Olah, G. A.; Ku, A.; White, A. M. *J. Org. Chem.* **1969**, *34*, 1827. (b) Olah, G. A.; White, A. M. *J. Am Chem. Soc.* **1968**, *90*, 6087.

(20) Berkessel, A.; Thauer, R. K. *Angew. Chem., Int. Ed. Engl.* **1995**, *34*, 2247.

(21) Hevesi, L.; Deasauvage, S.; Georges, B.; Evrad, G.; Blanpain, O.; Michel, A.; Harkema, S.; van Hummel, G. J. *J. Am. Chem. Soc.* **1984**, *106*, 3784.

(22) Atovmyan, L. O.; Ponomarev, V. I. *Zh. Strukt. Khim.* **1975**, *16*, 920.

(23) Lambert, J. B.; Schulz, W. J., Jr. *J. Am. Chem. Soc.* **1983**, *105*, 1671.

(24) Minkwitz, R.; Krause, R. Z.; Härtner, H.; Sawodny, W. *Anorg. Allg. Chem.* **1991**, *593*, 137.

(25) (a) The gas-phase ion−molecule reactions of $CH_3O(CH_2)_nSCH_3$ ($n = 1-3$) were investigated by pulsed ICR spectroscopy. The S-containing ion is formed preferentially over the O analogue: Pau, J. K.; Ruggera, M. B.; Kim, J. K.; Caserio, M. C. *J. Am. Chem. Soc.* **1978**, *100*, 4242. (b) According to stabilization energies, CH_2OH^+ is preferred by 2.3 kcal/mol over CH_2SH^+ but CH_2SMe^+ is preferred by 0.7 kcal/mol over CH_2OMe^+ at MP3/6-31G*//RHF/3-21G: Apeloig, Y.; Karni, M. *J. Chem. Soc., Perkin Trans. 2* **1988**, 625. (c) Modena, H.; Scorrano, G.; Venturello, P. *J. Chem. Soc., Perkin Trans. 2* **1979**, 3.

(26) Review of calculations of substituent effects of methyl cations (up to MP4SDTQ/6-31G*//6-31G*): Schleyer, P. v. R. *Pure Appl. Chem.* **1987**, *59*, 1647.

(27) (a) Stabilization of α-substituted methyl cations (R = H, NH_2, PH_2, OH, SH, F, Cl) at MP2/6-31G*//RHF/3-21G(*): Bernardi, F.; Bottoni, A.; Venturini, A. *J. Am. Chem. Soc.* **1986**, *108*, 5395. (b) RHF/3-21G studies of α-substituted carbocations show the ordering of stabilization as OH > SeH > SH: Rodriquez, C. F.; Hopkinson, A. C. *J. Mol. Struct. (Theochem)* **1987**, *152*, 55. (c) Stabilization of β-substituted ethyl cations and α-substituted methyl cations (R = H, Li, BeH, BH_2, CH_3, NH_2, OH, F, Na, MgH, AlH_2, SiH_3, PH_2, SH, Cl) at RHF/6-31G*: White, J. C.; Cave, R. J.; Davidson, E. R. *J. Am. Chem. Soc.* **1988**, *110*, 6308.

(28) $C(NH_2)_3^+$ and related systems: (a) Gonzalez, A. I.; Mo, O.; Yanez, M.; Leon, E.; Tortajada, J.; Morizur, J. P.; Leito, I.; Maria, P.-C.; Gal, J. F. *J. Phys. Chem.* **1996**, *100*, 10490. (b) Gobbi, A.; Frenking, G. *J. Am. Chem. Soc.* **1993**, *115*, 2362. (c) Jordan, M. J.; Gready, J. E. *J. Comput. Chem.* **1989**, *10*, 186.

(29) For a comparative study of tris(chalcogeno)carbenium ions $[C(XR)_3]^+$ (X = O, S, Se, Te), see: Ohlmann, D.; Marchand, C. M.; Grützmacher, H.; Chen, G. S.; Farmer, D.; Glaser, R.; Currao, A.; Nesper, R.; Pritzkow, H. *Angew. Chem., Int. Ed. Engl.* **1996**, *35*, 300.

by the topological analysis and, in addition, that this unexpected electronic motif persists even in the dication.

The ability of S to delocalize positive charge even in polycations is reflected in the facile oxidation of S_8 to S_8^{2+} by simply dissolving sulfur in concentrated H_2SO_4.[30] Heterocycles **V** (S/CH_2 exchange in S_x) can be oxidized to dications **VI** as well.[31] As in S_8^{2+}, transannular S−S bonds serve to delocalize positive charge thereby inducing excessive structural changes on going from the neutrals to the polycations. Other interesting cations with S−S bonds are obtained from electron rich disulfides. Again a considerable change in molecular geometry between the neutral $Me_2N-S-S-NMe_2$ (C_2) and its planar radical cation (C_{2h}) is observed.[32] Unsaturated ring systems with S atoms incorporated in the ring or as donor atoms in substituents can be oxidized and their products from redox processes are promising organic materials.[33]

In this context, the question arose as to whether thio groups SR may contribute to the stabilization of radical dications $[C(SR)_3]^{\bullet,2+}$ which can be derived by further oxidation of the monocations $[C(SR)_3]^+$. In this article, we report the results of an ab initio potential energy surface analysis of the monocation $[C(SH)_3]^+$ and of the parent radical dication $[C(SH)_3]^{\bullet,2+}$. The degenerate HOMO of $[C(SH)_3]^+$ is nonbonding in character and mainly located on the S atoms. Any structural change of molecular geometry upon oxidation is thus not easily predicted. The experimentally determined S−S distances in isolated trithiocarbenium ions (2.97−2.99 Å) are significantly less than twice the van der Waals radius of S (3.6 Å)[34] and we have searched for possible three-membered ring structures in which positive charge delocalization might occur via S−S bond formation. It is one of the goals of this study to examine whether cyclic distonic radical dication structures may compete energetically with non-distonic open structures. Minima and transition state structures for isomerization and automerization are reported for the monocation and the dication and the activation barriers to rotation provide a probe for the importance of Y-conjugation.[35] Structural and energetic effects of the second ionization of $[C(SH)_3]^+$ are evaluated. Topological electron density analysis is employed to analyze the interesting bonding situations in these cations. The electron density relaxation associated with the ionization process $[C(SH)_3]^+ \Rightarrow [C(SH)_3]^{\bullet,2+}$ has been examined and the ionization energy is reported. The neutral thioorthoacid $HC(SH)_3$, the precursor for the generation of $[C(SH)_3]^+$, has been considered as well and the hydride affinity of $[C(SH)_3]^+$ is reported. The mechanism by which the S substituents facilitate the generation of $[C(SH)_3]^+$ from $HC(SH)_3$ is analyzed quantitatively and in comparison to the unsubstituted parent system. Optimized structures are compared to available X-ray data of derivatives of these compounds to provide a reference for the adequacy of the reported geometries.

Theory and Computations

Restricted Hartree−Fock (RHF) and unrestricted Hartree−Fock theory[36] (UHF) were employed for the closed- and open-shell systems, respectively. While the wave functions obtained with the UHF formalism are eigenfunctions of the Hamiltonian and the $\mathbf{S}_z$ operators,[37] they are not eigenfunctions of the $\mathbf{S}^2$ operator. As a result, the wave functions of the doublet systems are spin contaminated to some extent by admixtures of quartet, sextet, and higher spin states.[38,39] The eigenvalues of the $\mathbf{S}^2$ operator are given as a measure of the spin-contamination. Since the projection operator commutes with the charge density operator,[40] the electron density remains unaffected by the projection and effects of spin contamination[41] on the optimized structures are expected to be small. Complete gradient optimizations of geometries were carried out within the point groups specified using the polarized split-valence basis set 6-31G*.[42] The Hessian matrix and vibrational frequencies were computed to characterize each stationary structure as a minimum or a transition state structure (or a higher-order saddle point) via the number of imaginary frequencies and to obtain vibrational information. The zero-point energies calculated at the HF level were scaled in the usual fashion[43] (factor 0.9) when applied to relative energies. Dynamic electron correlation between π- and σ-electrons is particularly important in conjugated molecules with a charged π-system and Borden and Davidson stressed the importance of triple excitations to correctly compute such systems.[44] In the present study, electron correlation effects on relative stabilities and reaction energies were estimated using full forth-order Mϕller−Plesset perturbation theory, including core electrons, and using the HF structures, MP4-(full,sdtq)/6-31G*//HF/6-31G*. For the open shell systems, spin contamination might have significant energetic consequences.[45,46] Annihilation of the first higher spin state removes the major part of the spin contamination and projection of the first three unwanted spin states results effectively in complete annihilation. The PMP4(s+3) energies are reported in a table in the Supporting Information. Pertinent relative energies are summarized in Table 1.

The electron and spin densities ρ and ρ^S are the sum and the difference, respectively, of the α and β electron density functions. We are analyzing both of these density functions without external reference

$$\text{electron density:} \qquad \rho = \rho_\alpha + \rho_\beta$$

$$\text{spin density:} \qquad \rho^S = \rho_\alpha - \rho_\beta$$

and solely based on properties of the electron density distribution. The topological analysis[47] is based on the properties of the gradient vector field. The collection of all gradient vector field lines originating at a given attractor defines the associated zero-flux surfaces as the boundaries of the atoms in the molecule. Bond critical points occur at the intersection between the zero-flux surfaces and the bond paths. A

(30) Gillespie, R. *J. Chem. Soc. Rev.* **1979**, *8*, 315.
(31) (a) Musker, W. K.; Wolford, T. L.; Roush, P. B. *J. Am. Chem. Soc.* **1978**, *100*, 6416. (b) Musker, W. K.; Roush, P. B. *J. Am. Chem. Soc.* **1976**, *98*, 6745. (c) Fujihara, H.; Akaishi, R.; Furukawa, N. *J. Chem. Soc., Chem. Commun.* **1987**, 930. (d) Dewello, T.; Lebrilla, C. B.; Asmus, K.-D.; Schwarz, H. *Angew. Chem., Int. Ed. Engl.* **1989**, *28*, 1275.
(32) Bock, H.; Schulz, W.; Stein, U. *Chem. Ber.* **1981**, *114*, 2623.
(33) (a) Heywang, G.; Roth, S. *Angew. Chem., Int. Ed. Engl.* **1991**, *30*, 176 and literature cited. (b) Klar, G.; Hinrichs, W.; Berges, P. *Z. Naturforsch. B* **1987**, *42*, 169. (c) Bock, H.; Rauschenbach, A.; Ruppert, K.; Havlas, Z. *Angew. Chem., Int. Ed. Engl.* **1991**, *30*, 714.
(34) (a) Bondi, A. *J. Phys. Chem.* **1964**, *68*, 441. (b) A critical value for weak covalent bonding interactions is derived from the SS distance of 2.60 Å in the S_4N_4 molecule. Wells, A. F. *Structural Inorganic Chemistry*, 5th ed.; Clarendon Press, Oxford, 1984, p 830.
(35) (a) Wiberg, K. B.; Laidig, K. E. *J. Am. Chem. Soc.* **1987**, *109*, 5935. (b) Ferretti, V.; Bertolasi, V.; Gilli, P.; Gilli, G. *J. Phys. Chem.* **1993**, *97*, 13568.
(36) Pople, J. A.; Nesbet, R. K. *J. Chem. Phys.* **1954**, *22*, 571.
(37) Musher, J. I. *Chem. Phys. Lett.* **1970**, *7*, 397 and references cited therein.
(38) See for example: Löwdin, P. O. *Quantum Theory of Atoms, Molecules, and the Soild State*; Academic Press, New York, 1966; p 601.
(39) Review: Karplus, M.; Rossky, P. J. *J. Chem. Phys.* **1980**, *73*, 6196.
(40) Nakatsuji, H.; Kato, H.; Yonezawa, T. *J. Chem Phys.* **1969**, *51*, 3175.
(41) (a) Glaser, R.; Choy, G. S.-C. *J. Phys. Chem.* **1993**, *97*, 3188. (b) Glaser, R.; Choy, G. S.-C. *J. Phys. Chem.* **1994**, *98*, 11379.
(42) (a) Hehre, W. J.; Ditchfield, R.; Pople, J. A. *J. Chem. Phys.* **1972**, *56*, 2257. (b) Hariharan, P. C.; Pople, J. A. *Theor. Chim. Acta* **1973**, *28*, 213. (c) Binkley, J. S.; Gordon, J. S.; DeFress, D. J.; Pople, J. A. *J. Chem. Phys.* **1982**, *77*, 3654.
(43) Hehre, W. J.; Radom, L.; Schleyer, P. v. R.; Pople, J. A. *Ab Initio Molecular Orbital Theory;* John Wiley & Sons, New York, 1986.
(44) Borden, W. T.; Davidson, E. R. *Acc. Chem. Res.* **1996**, *29*, 67.
(45) Löwdin, P. O. *Phys. Rev.* **1955**, *97*, 1509.
(46) (a) Schlegel, H. B. *J. Chem. Phys.* **1986**, *84*, 4530. (b) Gonzalez, C.; Sosa, C.; Schlegel, H. B. *J. Phys. Chem.* **1989**, *93*, 2435. (c) Chen, W.; Schlegel, H. B. *J. Chem. Phys.* **1994**, *101*, 5957.
(47) (a) Bader, R. F. W. *Atoms in Molecules—A Quantum Theory*; Clarendon Press, Oxford, United Kingdom, 1990. (b) Bader, R. F. W. *Chem. Rev.* **1991**, *91*, 893. (c) Bader, R. F. W. *Acc. Chem. Res.* **1985**, *18*, 9. (d) Bader, R. F. W.; Nguyen-Dang, T. T.; Tal, Y. *Rep. Prog. Phys.* **1981**, *44*, 893.

Table 1. Relative Energies

parameter	HF no proj.	ΔVZPE scaled	MP4 no proj.	PMP4 proj. s+3
I-Pref(**1b′** over **1b**)	0.56	−0.03	1.09	0.97
I-Pref(**1a** over **2a**)	2.13	−0.10	1.93	
I-Pref(**1b** over **2b**)	−1.36	0.11	−2.26	−1.84
I-Pref(**3b-t2** over **3b-t1**)	0.05	−0.03	−0.08	0.09
I-Pref(**3b-t2** over **3b-c2**)	1.09	0.07	0.73	0.88
I-Pref(**3b-c2** over **3b-c1**)	2.13	−0.29	1.71	1.57
I-Pref(**1b** over **3b-t2**)	46.31	0.85	35.49	42.05
E_A(**1a⟹4a**)	10.44	−0.34	9.51	
E_A(**1b⟹4b**)	5.15	−0.13	−2.73	3.46
E_A(**2a⟹4a**)	8.31	−0.24	7.58	
E_A(**2b⟹4b**)	6.51	−0.24	−0.47	5.30
E_A(**2a⟹5a-u**)	9.49	−0.18	8.64	
E_A(**2a⟹5a-w**)	8.92	−0.29	8.10	
E_A(**2b⟹5b-u**)	5.01	−0.16	−1.78	4.84
E_A(**2b⟹5b-w**)	10.00	−0.30	1.50	8.12
Pref(**1a** over **6a-I**)	68.98	−3.20	76.14	
Pref(**1a** over **6a-II**)	150.15	0.06	106.83	
Pref(**1a** over **6a-III**)	150.16	0.05	105.25	
Pref(**1b** over **6b**)	36.43	−1.95	56.27	58.97
IE(**1a→1b**)	335.82	−1.00	352.51	344.76
HA(**1a**)	267.75	−6.42	265.17	

[a] All values for isomer preference energies (I-Pref), activation energies (E_A), ionization energies (IE), and hydride affinity (HA) are in kcal/mol. [b] ΔVZPE terms calculated at the HF level are scaled (factor 0.9), and they are to be added to the relative energies.

bond path connects two attractors and is defined as the line traced out by following the direction of positive curvature of the electron density (λ_3). One first locates all bond critical points and then traces out the zero-flux surfaces following the directions associated with the two negative principal curvatures of the density, λ_1 and λ_2. Properties of the bond critical points such as the density at that point, ρ_b, and its distances r_A and r_B from the atoms, are commonly used to characterize electron density distributions and such information is collected in Table 2. Atomic properties are determined by integration within the basins. In Table 3, we report the integrated atomic Bader charges BC, the Bader populations associated with π-density BP(π), the spin populations SP, and the atom stabilities for the monocation **1a** and for the C_{3h} symmetric dication **1b**.

Calculations were performed with the program Gaussian94[48] and earlier versions on a network of IBM/RS-6000 systems, Silicon Graphics Indigo and PowerChallenge L computers, and Digital Equipment workstations. Electronic structures were examined at the HF/6-31G* level. Topological and integrated properties were determined with Extreme[49] and Proaim.[50] Cross sections of the electron densities were determined with Netz[51] and contoured with our PV-Wave programs.

Results and Discussion

Numbers refer to structures with different stereochemistry and the labels "**a**" and "**b**" are used to denote the cation and the dication, respectively. Total energies and vibrational properties are given as Supporting Information and relative energies are summarized in Table 1. The effects of spin annihilation and electron correlation both are important and Møller−Plesset energy calculations are not sufficient even when carried to full forth-order.[52] Unless otherwise noted, relative energies in the following refer to our highest level including projection of spin contamination, PMP4(full,sdtq)/6-31G*//HF/6-31G*+ΔZPE(HF/6-31G*).

Isomeric Open Structures and Pseudorotation of Jahn−Teller Distorted Dications. The C_{3h} structures **1a** and **1b** both are minima (Figure 1). While this symmetry is expected for **1a**, it is surprising for **1b** because the π-HOMO of **1a** is degenerate. Oxidation of **1a** removes this degeneracy, as shown in Figure 1, and results in an asymmetric wave function for **1b**. Symmetry reduction in the wave function allows for reduction in molecular symmetry and, hence, there might exist a second minimum for **1b** with lower symmetry due to Jahn−Teller distortion. Indeed, optimization within C_s symmetry leads to the structure **1b′**. At the UHF level, **1b′** is preferred over **1b** by 0.54 kcal/mol. Structure **1b′** is modestly distorted compared to **1b** in that the two C−S bonds adjacent to the smallest ∠(S−C−S) angle are elongated while the remaining C−S bond is shortened. The Jahn−Teller distorted structure **1b″** in which one C−S bond is elongated while the other two bonds are shortened corresponds to the transition state structure for pseudorotation.[53] At the MP4 and PMP4 levels very similar relative energies were predicted for **1b** and **1b′** which indicates that the pseudorotation of **1b′** is essentially unhindered and there is thus no need to optimize **1b″**.

The valence-MO diagrams of **1a** and of the isomers **1b** and **1b′** are shown in Figure 1. The RHF MOs are for **1a** and sets of α- and β-spin orbitals are shown for the radicals. For clarity, only the π-electrons are indicated by ↑ (α spin) and ↓ (β spin). Removal of one electron from the degenerate π-HOMO ($\pi_{27/28}$) results in a stabilization of the remaining unpaired π-electron (α-π_{26}) significantly below the energy of the remaining quasidegenerate π-HOMO (α-π_{28} and β-π_{27}) of the radical dication. The energies of the electrons of the all-bonding π_{23} MO in **1a** become greatly different in the dication (α-π_{23} and β-π_{24}). Most intriguing is the finding that *the unpaired electron is not in the HOMO of the dication*; instead, sets of spin paired π- and σ-electrons both are higher in energy compared to the MO associated with the unpaired π-radical. Dynamic electron correlation becomes so important in this charged radical because of this readily identifiable feature of the molecular orbitals.

Rotation about one of the C−S bonds in **1** leads to structures of type **2** for which the highest possible symmetry is C_s. The planar structures **2a** and **2b** are found to be minima. While **1a** is preferred over **2a** by 1.83 kcal/mol, we find a reversal of stability for the dication: **1b** is 1.73 kcal/mol less stable than **2b**.

The calculated structure of **1a** can be compared to the X-ray structure of $[C(SR)_3]^+$ with R = 2,4,6-triisopropylphenyl which realizes *de facto* C_{3h} symmetry of the central unit and good agreement is found for the C−S bond lengths. Ionization of **1a** hardly elongates the C−S (0.013 Å) and H−S (0.008 Å)

(48) *Gaussian94*, Revision C.3: Frisch, M. J.; Trucks, G. W.; Schlegel, H. B.; Gill, P. M. W.; Johnson, B. G.; Robb, M. A.; Cheeseman, J. R.; Keith, T.; Petersson, G. A.; Montgomery, J. A.; Raghavachari, K.; Al-Laham, M. A.; Zakrzewski, V. G.; Ortiz, J. V.; Foresman, J. B.; Cioslowski, J.; Stefanov, B. B.; Nanayakkara, A.; Challacombe, M.; Peng, C. Y.; Ayala, P. Y.; Chen, W.; Wong, M. W.; Andres, J. L.; Replogle, E. S.; Gomperts, R.; Martin, R. L.; Fox, D. J.; Binkley, J. S.; Defrees, D. J.; Baker, J.; Stewart, J. P.; Head-Gordon, M.; Gonzalez, C.; Pople, J. A. Gaussian, Inc.: Pittsburgh, PA, 1995.

(49) Biegler-König, F. W., McMaster University, Hamilton, Ontario, 1980.

(50) (a) Biegler-König, F. W.; Duke, F. A., McMaster University, Hamilton, Ontario, 1981. (b) Biegler-König, F. W.; Bader, R. F. W.; Tang, T.-H. *J. Comput. Chem.* **1982**, *3*, 317.

(51) Glaser, R., Department of Chemistry, University of Missouri−Columbia, 1990.

(52) See also: (a) Sekusak, S.; Guesten, H.; Sabljic, A. *J. Chem. Phys.* **1995**, *102*, 7504. (b) Donovan, W. H.; Famini, G. R. *J. Phys. Chem.* **1994**, *98*, 7811. (c) Arnaud, R.; Postlethwaite, H.; Barone, V. *J. Phys. Chem.* **1994**, *98*, 5913. (d) Bach, R. D.; Schlegel, H. B.; Andres, J. L.; Sosa, C. *J. Am. Chem. Soc.* **1994**, *116*, 3475. (e) Alvarez-Idaboy, J. R.; Eriksson, L. A.; Faengstroem, T.; Lunell, S. *J. Phys. Chem.* **1993**, *97*, 12737. (f) Corchado, J. C.; Olivares del Valle, F. J.; Espinosa-Garcia, J. *J. Phys. Chem.* **1993**, *97*, 9129. (g) Gonzalez, C.; Schlegel, H. B. *J. Am. Chem. Soc.* **1992**, *114*, 9118.

(53) The situation is closely related to $(H_2C)_3C^{\bullet+}$ and $C_6H_6^{\bullet+}$: (a) Trimethylenemethane radical cation: Du, P.; Borden W. T. *J. Am. Chem. Soc.* **1987**, *109*, 5330. (b) Benzene cation is D_{2d} symmetric but fluctional and best viewed as D_{6h} symmetric: Lindner, R.; Müller-Dethlefs, K.; Wedrum, E.; Haber, K.; Grant, E. R. *Science* **1996**, *271*, 1698.

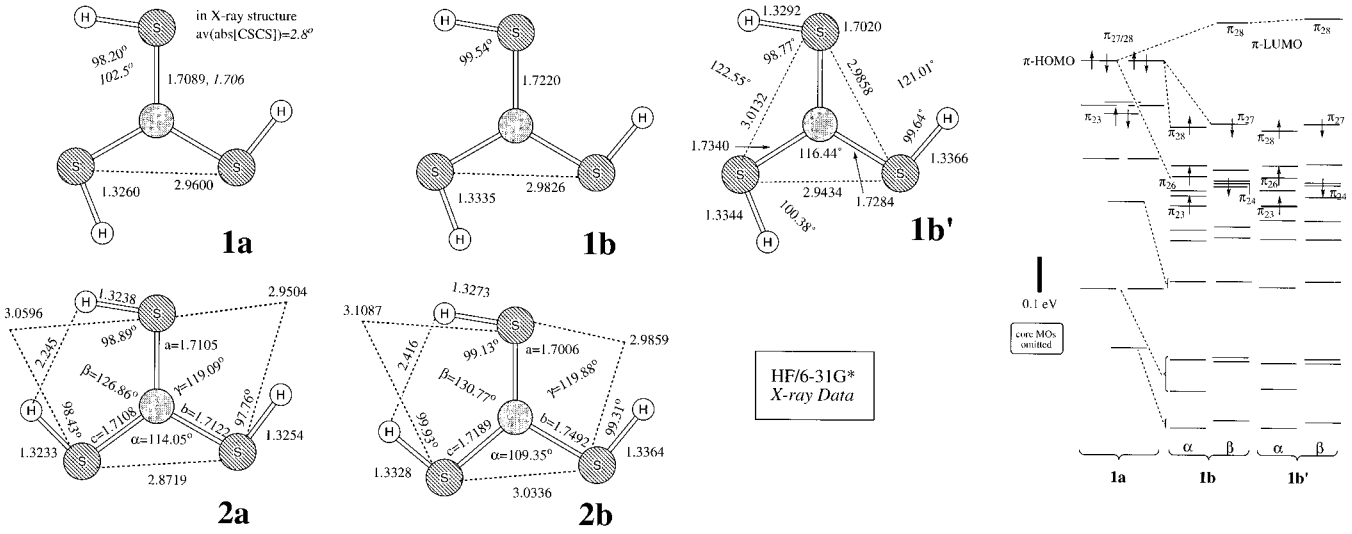

Figure 1. Structures of the minima C_{3h}-**1a** and C_s-**2a** of $[C(SH)_3]^+$. Structures **1b** (C_{3h}) and **1b′** (C_s) are minima for the dication $[C(SH)_3]^{\bullet,2+}$ resulting by oxidation of C_{3h}-**1a**. Dication C_s-**2b** is the oxidation product of **2a**. The MO diagrams are drawn to scale. Values given in italics for **1a** are the average X-ray data for $[C(SR)_3]^+$ with R = 2,4,5-triisopropylphenyl.

Scheme 2

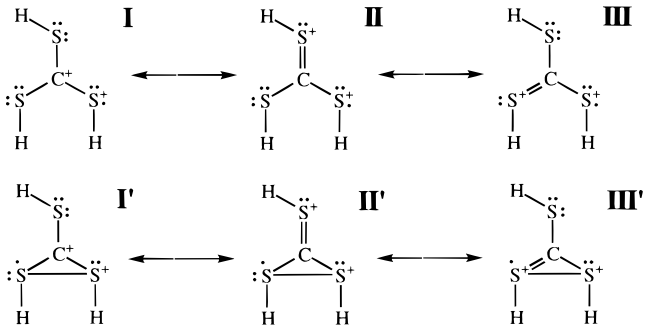

bonds and only a small reduction of the H−S−C angle (1.34°) occurs in **1b**. The C−S bonds in **2a** are on average 1.711 Å and modestly longer than in **1a**. For the dication, isomer **2b** differs from **1b** distinctly in that the *b* bond is elongated significantly while the *a* and *c* bonds (Figure 1) are shorter compared to C_{3h}-**1b**, suggesting that resonance form **III** has more weight than **II** (Scheme 2). To reduce nonbonded H−H repulsion, the β-angle is greatly increased in both cases and it is the α-angle (1,3 nonbonded S−S interaction) that is reduced while the γ-angle (affected by a nonbonded 1,4 S−H interaction) remains ≈120°.

Distonic Radical Cations with Ring Structures and Incipient Pyramidalization of the "Cationic" Carbon Center. In the open Lewis structures of the dication, some of which are shown in Scheme 2 for the type **2** structures (**I**−**III**), a formal positive charge and an unpaire electron need to be placed at the same S atom. No resonance forms are available without an "S radical cation". Lewis structures with S atoms that carry either a formal positive charge or an unpaired electron, but not both, can only be written if S−S bond formation occurs to form cyclic structures (e.g. **I′** and **II′**). These ring structures are *distonic* radical cations.[54] The advantage of distonic radical cations is simply that the total number of unpaired and lone pair electrons is minimized. Distonic radical cations were shown to be responsible for the facile oxidation of 1,3-dithianes[55] and the formation of the distonic radical cation from thiirane radical cations via the electrocyclic ring-opening reaction has been suggested.[56] In the case of the dication, the question arises whether this advantage suffices to compensate for the ring strain energy associated with the S−S bond formation.

We searched the potential energy surface for such a structure and, indeed, several bridged chiral stereoisomers of **3b** were located (Figure 2) and found to be local minima. In both "cis isomers" **3b-c1** and **3b-c2**, the endocyclic S−H bonds are *cis* with regard to each other. While in **3b-c1** both S−H bonds are *cis* with regard to the exocyclic C−S bond, they are *trans* in **3b-c2**. These "*cis* isomers" are not simple rotamers about the exocyclic C−S bond, but they have different configurations at the central C atom. In the "*trans* isomers" **3b-t1** and **3b-t2**, the endocyclic S−H bonds are *trans* to each other. In **3b-t1** and **3b-t2**, the ring H that is *syn* or *anti* with the exocyclic H−(S) is *trans* with regard to the exocyclic C−S bond, respectively.

Isomer **3b-t2** is the most stable of these bridged structures. For all practical purposes, the *trans* structures **3b-t1** and **3b-t2** are isoenergetic. **3b-c2** is 1.22 kcal/mol less stable than **3b-c1**. The most stable isomer of **3b**, **3b-t2**, is 42.90 kcal/mol less stable compared to C_{3h}-**1b**. The S−S bond formation leading to the distonic radical is thus impeded by the concomitant increase in ring strain. Our results predict that ring structures are thermodynamically disfavored compared to the open structures.

The S−S bonds in *cis* and *trans* **3b** are 2.107 ± 0.004 and 2.098 ± 0.001 Å, respectively. For comparison, the S−S bond in *gauche* (89.8°) HS−SH is 2.0631 Å at the same theoretical level. We optimized the protonated derivative, C_s HS−SH_2^+, and an S−S bond length of 2.082 Å was found. The comparisons indicate that the S−S bond in **3b** is slightly weakened due to electron deficiency. Significant contributions from **II′** are indicated since the exocyclic C−S bond is rather short, only 1.686−1.693 Å, while the C−S bonds in the ring are long (average 1.776 Å) compared to **1b** and **2b**. An interesting feature of all ring structures of **3b** concerns the substantial pyramidalization at carbon. The electron-deficient trivalent carbon intrinsically prefers trigonal-planar hybridization but the carbon pyramidalization might serve in this case to reduce strain associated with the CS_2 ring.

Effects of Oxidation on Rotational Isomerizations—Probing C−S Conjugation. The isomerization between **2** and **1**

(54) (a) Yates, B. F.; Bouma, W. J.; Radom, L. *J. Am. Chem. Soc.* **1984**, *106*, 6805. (b) Radom, L.; Bouma, W. J.; Nobes, R. H.; Yates, B. F. *Pure Appl. Chem.* **1984**, *56*, 1831.

(55) Glass, R. S. *Main Group Chem. News* **1994**, *2(3)*, 4.

(56) Kamata, M.; Miyashi, T. *J. Chem. Soc., Chem. Commun.* **1989**, 557.

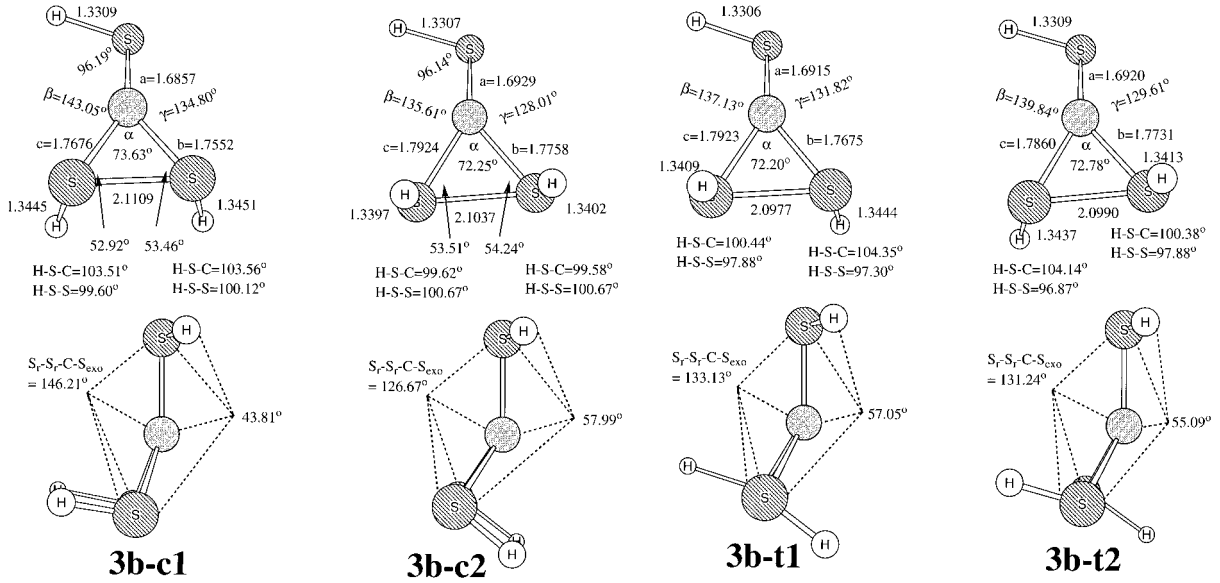

Figure 2. Four stereoisomers of the three-membered ring structure **3b** are local minima of the dication $[C(SH)_3]^{\bullet,2+}$.

involves rotation about the *c* bond of **2** indicated in Figure 1 and proceeds along enantiomerically related pathways via the chiral transition state structures **4a** and **4b**.[57] Rotation about the *a* or *b* bonds in **2a** or **2b** results in automerization via the C_s-symmetric transition state structures **5a** and **5b** (Figure 3). The structures **5** come as isomers **5-w** and **5-u** depending on whether rotation occurs about the *a* or the *b* bond, respectively. The labels "w" and "u" describe the shape of the in-plane H−S−C−S−H fragment. Bond rotation in **1** via **4** or **5** leaves the trigonal-planar carbon sp^2 hybridization intact and the H−C−S angles of the "in-plane" SH groups are affected little. The C_{3v} symmetric structures **6a** and **6b** were optimized to examine the effects of having *all* S−H bonds in conformations that are not suitable for S→C π-dative bonding. For **6a**, three such structures were found. **6a-I** is the most stable structure of these, and it exhibits three imaginary frequencies that all are associated with rotations about C−S bonds. The structures **6a-II** and **6a-III** are second-order saddle points and their CS_3 units are distinctly pyramidalized (Figure 3) at carbon as the result of the S−C density shift realized in their common electronic configuration. **6a-II** and **6a-III** differ in that the H atoms and the C atom are on the same or opposite sides, respectively, of the S_3 plane. These structures are isoenergetic at the level of optimization and distortions along the CS_3 inversion coordinate require little energy. The model **6a-90** in which a trigonal-planar C atom was forced gave a slightly higher energy (0.3 kcal/mol) at the level of optimization. In the case of the dication, we also obtained several stationary structures, and we report the structure that is most stable at the level of optimization. This structure **6b** (Figure 3) is a transition state with a slight degree of C-pyramidalization. These calculations of the model structures **6** suggest an interesting proposition: It might be possible to realize C-pyramidalization in carbenium ions by providing an incentive for a face-preference through hyperconjugation.

The lengths of the C−S bonds that are being rotated in **4a** and **4b** are 1.796 and 1.831 Å and they are much longer than in **1a** (by 0.09 Å) and **1b** (by 0.11 Å) while the remaining C−S bonds are shortened by ≈0.026 Å in **4a** and ≈0.042 Å in **4b**. The same is true and slightly more pronounced for **5a** and **5b**. For **4a** and **4b**, these are the kinds of structural effect one would expect for a change in conjugation associated with bond rotation. Similarly, one would be tempted to predict longer bond lengths for all C−S bonds in **6a** and **6b**, but this is only the case for **6a-I** and **6b** and *not* for **6a-II** and **6a-III**. In **6a-II** and **6a-III**, the C−S bonds are actually shorter than in **1a** and this shortening is more pronounced for **6a-III**.

Figure 3 shows the great similarities in the *structural characteristics* of the potential energy surfaces of the cation and the dication. Yet, there are some significant differences in the *energetics*. Schematic and to scale representations of the potential energy surfaces of the cation $[C(SH)_3]^+$ and the dication $[C(SH)_3]^{\bullet,2+}$ are summarized in Figure 4. At the PMP4 level, the activation barriers for the processes **1a** ⟹ **4a**‡ and **1b** ⟹ **4b**‡ are 9.17 and 3.33 kcal/mol, respectively. These computed rotational barriers are comparable to the activation barriers of 8−14 kcal/mol measured for some disubstituted systems $[RC(SR)_2]^+$.[21] For the automerizations **2a** ⟹ **5a-u**‡ ⟹ **2a** and **2a** ⟹ **5a-w**‡ ⟹ 2**a**, the activation barriers are 8.46 and 7.81 kcal/mol, respectively, at the highest level. For the automerizations of **2b** via **5b-u**‡ or **5b-w**‡, the activation barriers are 4.68 and 7.82 kcal/mol, respectively. One would have expected that the rotational processes in the dication are less hindered than in the monocation. This is true for the isomerizations via **4** and for most automerizations but not for the automerization via **5b-w**‡. The automerization of **1** involves a sequence of isomerizations to **2** via **4**‡ and automerizations of **2** via **5**‡ and the former isomerizations are rate-limiting for the monocation while the latter is rate-limiting for the dication. The relative energies of the models C_{3v}-**6** as compared to C_{3h}-**1** are large: The most stable structure of **6a** is more than 79 kcal/mol less stable than **1a** and **6b** is 61 kcal/mol less stable than **1b**. The relative stabilities of **6a** and **6b** are much higher than three times the value of the respective activation barriers to rotation, that is, the loss of one S→C donation in the transition state structure for C−S rotation is effectively counteracted by increased S→C donation in the two other C−S bonds.

Factors Affecting the Hydride Affinity of Trithiocarbenium Ion: Methane Destabilization and Cation Stabilization. While there have been several theoretical studies of the lighter

(57) The electron configuration of the structure **4b** discussed in the text contains a near-planar HS−C−SH 4-e-π-system and the "rotated SH" group is oxidized. We also optimized a transition state structure **4b** with a HS−C−SH 3-e-π-system and a shorter C−S bond involving the rotating SH group. The energies of this structure **4b-3**π are as follows: *E*(UHF) = −1231.307308; VZPE = 22.44; *E*(MP4(sdtq)) = −1231.861778; *E*(PUHF(*s*+1)) = −1231.329366; *E*(PUHF(*s*+3)) = −1231.327587; *E*(PMP4(*s*+3)) = −1231.876861.

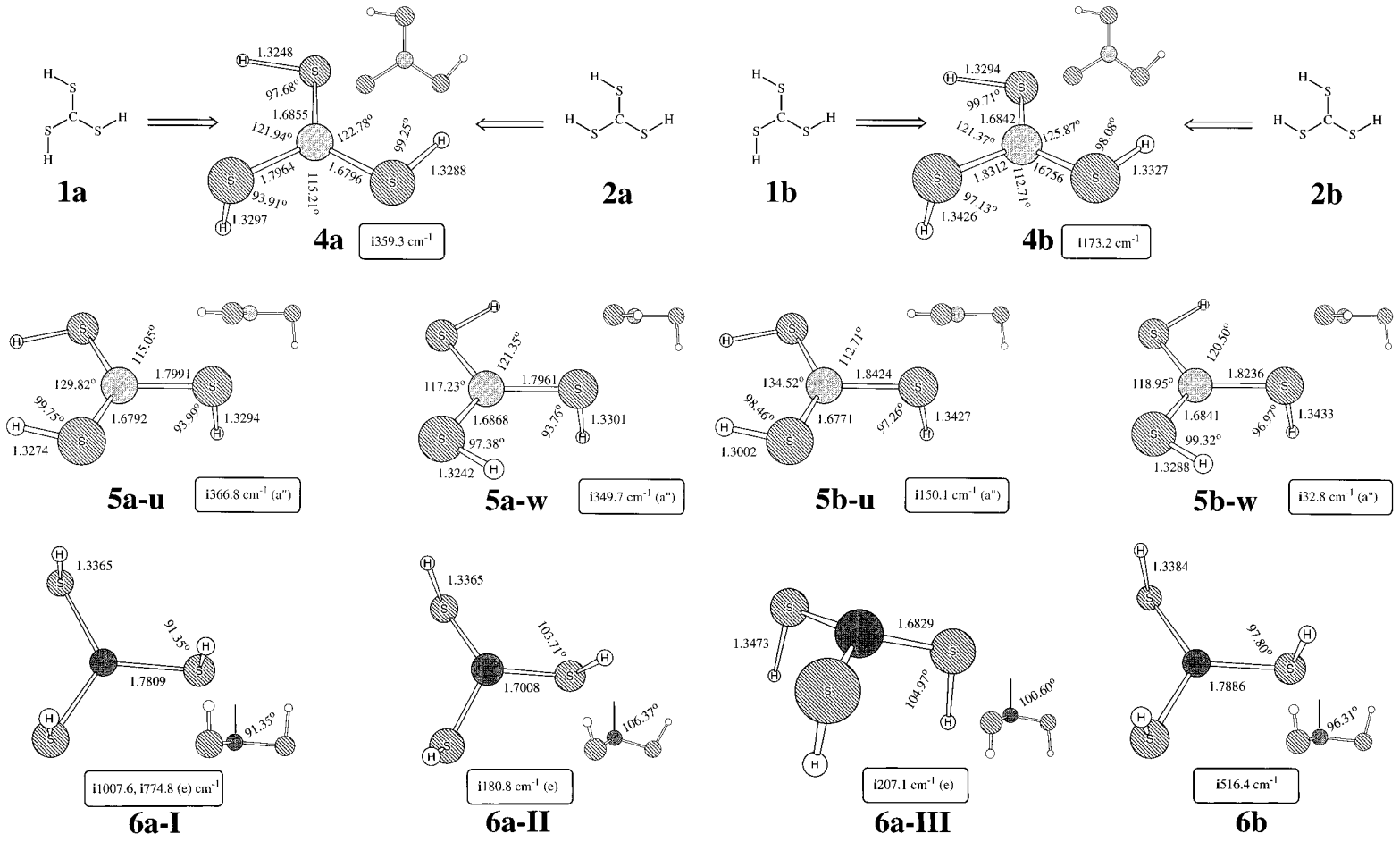

Figure 3. The transition state structures for isomerization **1** ⟹ **4**‡ ⟹ **2** and automerizations **2** ⟹ **5-u**‡ ⟹ **2** and **2**⟹ **5-w**‡ ⟹ **2** are shown for the monocation (left) and the dication (right). Model structures **6** correspond to higher-order saddle points.

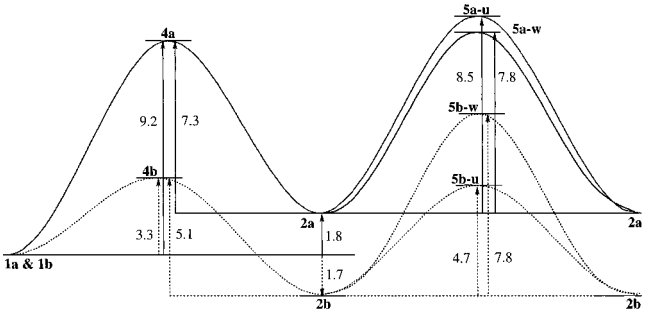

Figure 4. The potential energy surface diagram is shown for the monocation (solid) and the dication radical (dashed). The potential energy diagram is represented to scale as computed at the PMP4/6-31G*//HF/6-31G*+ΔVZPE level.

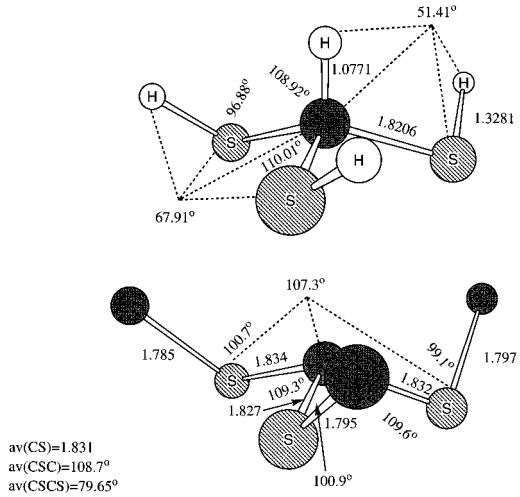

Figure 5. The optimized structure of $HC(SH)_3$ and comparison to the X-ray structure of $HC(SR)_3$ with R = 2,4,6-triisopropylphenyl.

homologue,[58,59] it appears that the neutral molecule $HC(SH)_3$ has not been studied. We optimized $HC(SH)_3$ in C_3 symmetry[60] with *s-cisoid* H−C−S−R conformations (Figure 5) and the resulting equilibrium geometry **1-H** agrees well with the crystal structure of the analog $HC(SR)_3$ (R = 2,4,6-*i*$Pr_3C_6H_2$). The formation of **1a** from **1-H** via heterolytic C−H bond dissociation (eq 1) requires 261.3 kcal/mol at the RHF/6-31G* level. This

$$HC(SH)_3\ (\mathbf{1\text{-}H}) \rightarrow H^- + [C(SH)_3]^+\ (\mathbf{1a}) \qquad (1)$$

value for the hydride affinity (HA) is expected to be too high since a proper functional description of hydride ion requires diffuse functions and eq 1 was evaluated also with the 6-31++G** basis set. At the MP4(full,sdtq)/6-31++G**//RHF/6-31G* level and including scaled VZPE(RHF/6-31G*), HA(**1a**) becomes 217.7 kcal/mol. The hydride affinity of methyl cation is $HA(CH_3^+)$ = 313.2 kcal/mol.[61a] The difference between the hydride affinities of **1a** and CH_3^+ provides a quantitative measure for the increased propensity of the trithio-

Scheme 3

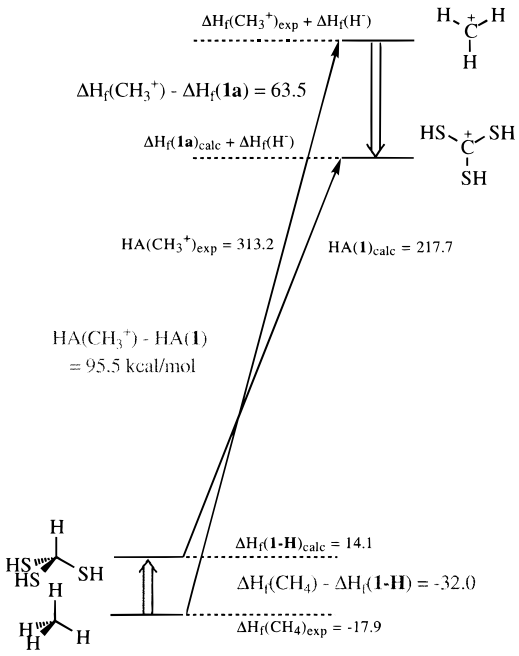

substituted system to form the cation and HA(**1-H**) is about 95.5 kcal/mol lower compared to the respective value for methane.

The heat of formation ΔH_f(**1a**) can be determined via the reaction enthalpy of the isodesmic reaction shown in eq 2—ΔH_r = −101.12 kcal/mol including scaled vibrational zero-point

$$CH_3^+ + 3CH_3SH \rightarrow 3CH_4 + [C(SH)_3]^+\ (\mathbf{1a}) \qquad (2)$$

energies—and with $\Delta H_f(CH_3SH)$ = −5.34 kcal/mol one finds ΔH_f(**1a**) = 197.72 kcal/mol. ΔH_f(**1-H**) can be determined with the heats of formation of **1a** and H^- in combination with the computed HA(**1a**) of eq 1 and a value of ΔH_f(**1-H**) = 14.1 kcal/mol is obtained. The thermochemical relations are represented schematically and to scale in Scheme 3. The formation of the trithio-substituted cation is facilitated both by an increase in the enthalpy of the neutral substrate and by an increased cation stability. The large difference in the hydride affinities of methyl cation and **1** results from a *destabilization of the neutral derivative* **1-H** by 32.0 kcal/mol and a greater *stabilization of the cation* **1a** by 63.5 kcal/mol. Both modes of substituent action are important and the latter is nearly twice as large. Steric crowding in the neutral trithio compound by means of SR substituents instead of the model SH groups should raise ΔH_f-(**1-R**) and the computed reduction in the HA value of **1-H** thus should be taken as a lower limit for the stabilization that can be achieved with compounds of type **1-R**.

Ionization Potential of Trithiocarbenium Ion. Ionization potentials (IP) for the process **1a** → **1b** + e^- were determined using Koopmans' theorem[62] and directly with the energies of

(58) $HC(OH)_3$: (a) Lathan, W. A.; Radom, L.; Hehre, W. J.; Pople, J. A. *J. Am. Chem. Soc.* **1973**, *95*, 699. (b) Lehn, J.-M.; Wipff, G.; Bürgi, H.-B. *Helv. Chim. Acta* **1974**, *57*, 493. (c) Ree, A. E.; Schade, C.; Schleyer, P. v. R.; Kamath, P. V.; Chandrasekhar, J. *J. Chem. Soc., Chem. Commun.* **1988**, 67. (d) Böhm, S.; Senf, I.; Schädler, H.-D.; Kuthan, J. *J. Mol. Struct. (Theochem)* **1992**, *253*, 73.

(59) $HC(OCH_3)_3$: (a) Spelbos, A.; Mijlhoff, F. C.; Faber, D. H. *J. Mol Struct.* **1977**, *41*, 47. (b) Aped, P.; Fuchs, B.; Goldberg, I.; Senderowitz, H.; Tartakovsky, E.; Weinman, S. *J. Am. Chem. Soc.* **1992**, *114*, 5585.

(60) The C_3-symmetric structure was considered as a model of the solid state structure of the derivative. The most stable structure of $HC(SH)_3$ is non-symmetric (C_1) and contains two *gauche* and one *anti* H−S−C−H arrangements.

(61) (a) Based on $\Delta H_f(CH_4)$ = −17.9 kcal/mol,[61b] $\Delta H_f(CH_3^+)$ = 261.2 kcal/mol,[61c] and $\Delta H_f(H^-)$ = 34.1 kcal/mol (half the homolytic bond dissociation energy[61d] of H_2 of 103 kcal/mol minus the H electron affinity[61e] of 0.7542 eV.[61f] (b) Lide, D. R. *CRC Handbook of Chemistry and Physics*, 71th ed.; CRC Press, Baton Rouge, 1990; pp 5−74. (c) Traeger, J. C.; McLoughlin, R. G. *J. Am. Chem. Soc.* **1981**, *103*, 3647. (d) Janz, G. J. *Thermodynamic Properties of Organic Compounds*; Academic Press: New York, 1967. (e) Hotop, H.; Lineberger, W. C. *J. Phys. Chem. Ref. Data* **1985**, *14*, 731. (f) Reported values for $HA(CH_3^+)$ vary somewhat: Hydride affinity of 312.2 kcal/mol reported for methyl cation: Screttas, C. G. *J. Org. Chem.* **1980**, *45*, 333.

(62) Szabo, A.; Ostlund, N. S. *Modern Quantum Chemistry: Introduction to Advanced Electronic Structure Theory;* Macmillan Publising Co.; New York, 1982, p 127.

Table 2. Topological Properties of **1a**, **1b**, and **1b′**

atoms	r_A	r_B	F	ρ	λ_1	λ_2	λ_3	ϵ
				***C*$_{3h}$-1a**, RHF				
C−S	1.114	0.642	0.634	0.214	−0.297	−0.170	0.357	0.742
S−H	0.877	0.449	0.661	0.222	−0.489	−0.452	0.307	0.081
				***C*$_{3h}$-1b**, UHF (and PUHF)				
C1−S2	0.912	0.809	0.530	0.223	−0.347	−0.294	0.061	0.181
C1−S3	0.905	0.817	0.526	0.223	−0.350	−0.296	0.070	0.180
C1−S4	1.071	0.651	0.622	0.206	−0.273	−0.154	0.312	0.765
S2−H5	0.922	0.411	0.692	0.224	−0.535	−0.523	0.375	0.022
S3−H6	0.915	0.418	0.686	0.225	−0.527	−0.514	0.347	0.024
S4−H7	0.899	0.434	0.675	0.220	−0.500	−0.469	0.340	0.067
				***C*$_s$−1b′**, UHF (and PUHF)				
C1−S2	1.063	0.639	0.624	0.210	−0.281	−0.163	0.411	0.723
C1−S3	0.900	0.827	0.521	0.222	−0.349	−0.298	0.084	0.169
C1−S4	0.888	0.845	0.512	0.219	−0.348	−0.300	0.106	0.162
S2−H5	0.896	0.433	0.674	0.222	−0.506	−0.475	0.337	0.064
S3−H6	0.924	0.412	0.692	0.223	−0.529	−0.518	0.376	0.022
S4−H7	0.916	0.418	0.686	0.224	−0.526	−0.513	0.369	0.025

[a] Parameters r_A and r_B are the distances of the bond critical point (BCP) from the atoms A and B specified in the first column in Å; $F = r_A/(r_A + r_B)$; ρ is the value of the electron density at the BCP (in e au^{-3}), λ_i are the principal curvatures of ρ at the BCP, and the ellipticity is derived *via* $\epsilon = \lambda_n/\lambda_m - 1$, where $\lambda_n < \lambda_m$ and $\lambda_i < 0$.

1a and **1b**. With ϵ(HOMO,**1a**) = −0.59258 au Koopmans' theorem predicts IP(**1a**) = 371.9 kcal/mol (16.1 eV). This approximation neglects the relaxation of the remaining electrons after ionization of **1a** and usually represents *an upper limit* of the true IP although correlation effects counteract. Direct evaluation of the ionization potential at the HF/6-31G* level and considering $\upsilon = 0$ yields IP(**1a**) = 334.8 kcal/mol (14.5 eV). This value should be *a lower limit* since **1a** and **1b** are computed using RHF and UHF theory, respectively. A great improvement in the accuracy of the IP can be achieved when these wave functions are used as references in the full forth-order Møller−Plesset treatment. At the PMP4(full,sdtq)/6-31G*//HF/6-31G* level and considering the ZPE differences at the HF level one obtains IP(**1a**) = 343.8 kcal/mol (14.9 eV). With this best estimate for IP(**1a**) and with ΔH_f(**1a**) = 197.7 kcal/mol, we derive ΔH_f(**1b**) = 541.5 kcal/mol.

Inductive and Conjugative S→C Polarizations in "Trithiocarbenium Ions". In valence bond theory, the monocation **1a** is described by the resonance form that corresponds to the trithio-substituted carbenium ion and by the set of the triply degenerate resonance forms in which the positive charge is delocalized onto S by S-lone pair donation toward C. Based on these *formal* charges in the Lewis structures describing Y-conjugation,[63] one might be inclined to assume that the positive charge is well distributed over all the heavy atoms of **1a**. The resonance forms do not reflect actual charges and the topological electron density analysis reveals a different picture. The S atoms are electron-deficient indeed but the sum of the SH group charges of +0.750 far exceeds unity: A negative charge of q(C) = −1.248 is revealed for the "electron-deficient" carbon! The Bader π-populations BP(π) show that the SH groups donate π-density to carbon (0.309 each) as suggested by the respective resonance forms. The electron density analysis shows that there also is a strong polarization in the σ-system that leads to density accumulation at C at the expense of the SH groups. To reflect this electron density feature in Lewis notations, it becomes necessary to employ CS non-connected valence bond structures in which the C−S σ-bond electron pair

Scheme 4

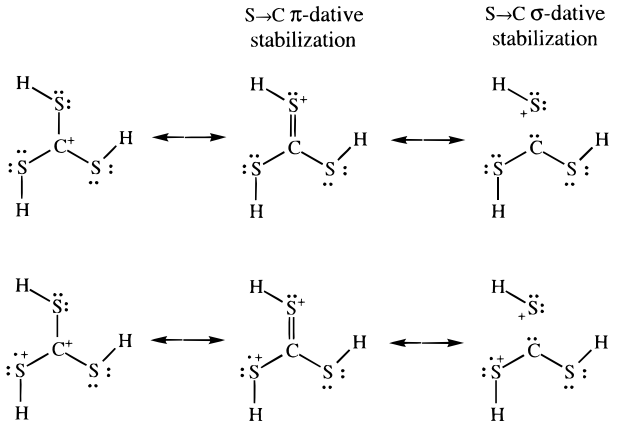

Scheme 5

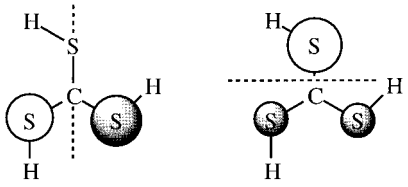

is assigned to C (top row in Scheme 4).[64] Clearly, the name "trithiocarbenium ion" does not adequately describe the electronic structure. The electronic structure of **1a** indicates that nature tends not only to disperse positive charge to the periphery of the Y-shaped system, but to polarize the C−S bonds in such a way as to create a negative center.[65] Apparently, there is an electrostatic advantage associated with placing larger positive charges around a negatively charged center compared to just distributing the positive charge.

Oxidation of **1a** removes one electron from one of the π-HOMOs and results in **1b**. The HOMOs of **1a** are schematically shown in Scheme 5 where the approximate node planes are indicated as dashed lines. The graphical depictions of the electron and spin density distributions (*vide infra*) show that oxidation occurs for the MO sketched on the left and denoted HOMO'. This oxidation causes a so-called fragment-inequality[2b] since the equivalence of the SH groups vanishes. The removal of one electron from HOMO′ leaves one SH fragment relatively unchanged (the one on the node or close to it) and there exist three degenerate electronic states for **1b** since it is equally probable for each SH fragment to be this least affected SH fragment. In other words, the electronic structure of **1b** can be realized in three ways and there also are three structures **1b′** depending on which of the three C−S bonds is elongated. The three states are vibronically coupled and the transitions from one state to another are associated with intramolecular charge and spin transfer between the SH fragments. The potential energy surface analysis shows that the energy gain due to the Jahn−Teller effect in **1b′** is small. Consequently, the pseudorotation between the *three* **1b′** structures is facile and we will focus on the average properties in our discussion of the integrated properties. The ESR spectra, for example, can be

(63) For discussions of resonance interactions on Y-conjugated systems, see: (a) Wiberg, K. B. *J. Am. Chem. Soc.* **1990**, *112*, 4177. (b) Horn, H.; Ahlrichs, R. *J. Am. Chem. Soc.* **1990**, *112*, 2121. (c) Ogorodnikova, N. A. *J. Mol. Struct.* **1993**, *301*, 189.

(64) (a) The need for non-connected Lewis structures for the description of dative bonding in diazonium ions has been discussed in ref 11. (b) For interpretations of electron density distributions using Lewis structures, see also: Glaser, R.; Murmann, R. K.; Barnes, C. L. *J. Org. Chem.* **1996**, *61*, 1047.

(65) For a discussion of the dominance of electrostatics in multiple bonding involving second-row elements, see: Rajca, A.; Lee, K. H. *J. Am. Chem. Soc.* **1989**, *111*, 4166.

Table 3. Integrated Properties for **1a** and **1b**

	cation **1a** at RHF			dication **1b** at UHF					dication **1b** at PUHF	
atom	BC	BP(π)	energy	BC	BP(π)	SP	SP(π)	energy	BC	SP
C1	−1.248	0.926	−38.371152	−0.901	1.104	−0.265	−0.195	−38.099034	−0.853	−0.057
S2	0.641	1.668	−397.286380	0.775	1.143	0.787	0.729	−397.257588	0.759	0.569
H5	0.109	0.023	−0.541290	0.238	0.011	−0.016	0.007	−0.483706	0.238	−0.002
S3				0.795	1.141	0.789	0.731	−397.248136	0.779	0.573
H6				0.208	0.015	−0.016	0.008	−0.497194	0.208	−0.002
S4				0.723	1.568	−0.282	−0.278	−397.223166	0.703	−0.083
H7				0.168	0.019	0.003	−0.004	−0.511035	0.169	0.001
Σ	1.002	5.999	−1231.854162	2.003	5.002	1.000	0.998	−1231.319859	2.003	0.999
S2H5	0.750	1.691	−397.827670	1.013	1.154	0.771	0.736	−397.741294	0.997	0.576
S3H6				1.003	1.156	0.773	0.739	−397.745330	0.987	0.571
S4H7				0.888	1.587	−0.279	−0.282	−397.734201	0.872	−0.082

[a] Integrated Bader charge (BC) and Bader populations (BP), spin population (SP), and atom energy ($E = -E_{kin}$). [b] Difference between integrated and directly computed molecular energy for **1a** and **1b** (UHF) is 0.009 and 0.53 kcal/mol, respectively.

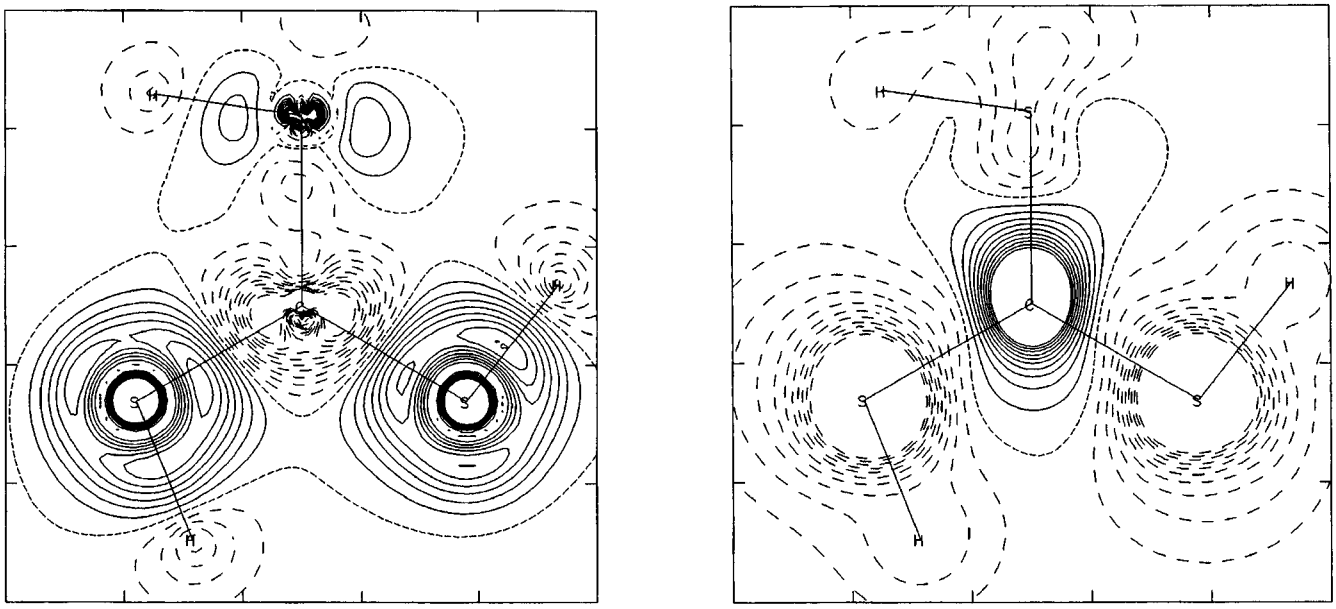

Figure 6. Electron density difference function $\Delta\rho = \rho^{PUHF}([C(SH)_3]^{\bullet,2+}) - \rho^{RHF}([C(SH)_3]^{+})$ as computed with the HF/6-31G* structure of the monocation C_{3h}-**1a**. Contour increments are 2×10^{-3} e au^{-3} for $\Delta\rho$ in the molecular plane (left) and they are 10^{-3} e au^{-3} for the cross section in a plane parallel to the molecular plane and 0.5 Å away from it.

expected to describe the average spin density distribution of the three radical dications **1b′**. The structural differences between **1b** and **1b′** are marginal and we examined the electronic structure of the radical dication using the **1b** structure.

Integrated properties for **1b** were determined both with the UHF and with the PUHF densities (Table 3). Spin projection has only a small effect on the electron density distribution and we will discuss the UHF electron densities as they allow for σ/π separation which is advantageous for conceptual reasons. Based on the valence-bond description of **1b**, one would expect that oxidation of **1a** leads to removal of electron density from the S atoms and this is true to a certain degree. The total charge of all SH groups is increased from 2.25 in **1a** to 2.90 in **1b**. At the same time, the C population is reduced by 0.35 but the carbon atom remains negatively charged even in the dication! The *electronic motif of placing large positive charges around a central negative center persists.* As the S atoms become more electron deficient in going from **1a** to **1b**, their electronegativity increases and the C←S polarization is somewhat reduced. The π-populations of the SH groups overall decrease by *more than one electron*, that is, the carbon's π-population increases by 0.18. *Oxidation overall removes electron density from the central carbon while it also renders this atom more* π-acidic. As with the monocation, it becomes evident that the electronic structure of the dication is best interpreted considering Lewis structures describing the S→C π- and σ-donation in which one of the SH groups is singly oxidized (bottom row in Scheme 4).

The electronic relaxations associated with adiabatic oxidation are clearly manifested in the electron density difference (EDD) function $\Delta\rho$. This function is defined as the difference between the electron density functions $\rho(C_{3h}$-**1b**) and $\rho(C_{3h}$-**1a**) and its computation is based on the structure of C_{3h}-**1a**. The plots of $\Delta\rho$ shown in Figure 6 were determined using the PUHF density of C_{3h}-**1b** which is essentially the same as the UHF density since the spin projection operator commutes with the electron density operator. Removal of an electron from the π-HOMO′ causes strong polarization in the σ-system. The negative contours in the carbon region show the *reduction* of carbon σ density and an *increase* of σ electron density in the S regions (Figure 6, left). This C→S electron density shift reflects the increase of the S electronegativity upon oxidation and counteracts the S→C π density shift (Figure 6, right).

Strong Spin Polarization in the σ-System. While the UHF and PUHF electron density distributions differ only marginally, the associated spin density functions differ greatly and the PUHF spin density is superior to the UHF spin density function.[41] We discuss the spin populations determined with the PUHF wave function and the cross sections of the spin density function $\rho^{S,PUHF}$ of C_{3h}-**1b** are shown in Figure 7 in the same cross sections as with the electron density difference plots. The

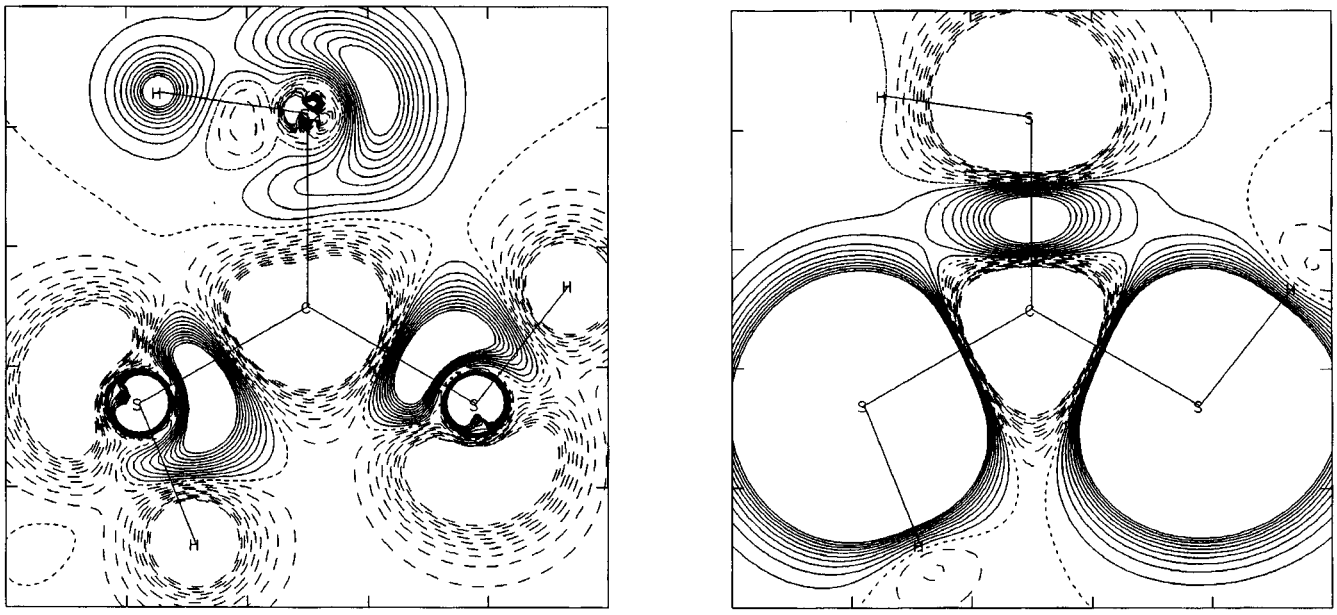

Figure 7. Cross sections of the spin density function $\rho^{S,PUHF}([C(SH)_3]^{\bullet,2+})$ are shown for the molecular plane (left) and for a plane parallel to the molecular plane and 0.5 Å away from it (right). Contour increments are 10^{-4} α e au^{-3}.

HOMO′ of **1a** becomes singly occupied in **1b** and, consequently, two S atoms show large α-spin densities in the π-system. The C atom is assigned β-spin density due to spin polarization. Interestingly, the unique S does not show α-spin density excess in the π-system. Instead, there occurs a region of α-spin excess in the unique C−S bond region but β-spin density at that S atom. The π-hole causes strong spin polarization in the σ-system as is clearly evidenced in the plot shown to the left in Figure 7. We pointed out above that the MO of the unpaired electron is *not* the HOMO of the dication but that sets of spin-paired π- and σ-electrons are less bonding than the MO associated with the unpaired π-radical and the strong spin polarization observed therefore comes as no surprise. The C atom shows β-spin density in the σ-system as well. For the SH groups, we find β-spin density in the S lone pair region and in the S core region, and areas of α-spin density in the S−H and S−C bonding regions. The spin density difference function $\Delta\rho^S = \rho^{PUHF}([C(SH)_3]^{\bullet,2+}) - \rho^{UHF}([C(SH)_3]^{\bullet,2+})$ of C_{3h}-**1b** also was computed to examine the effects of annihilation of spin contaminants in the UHF density. The resulting plot in the molecular plane greatly resembles the pattern found in the left plot in Figure 7. The function $\Delta\rho^S$ assumes positive values in all areas in which the spin density indicates β-density and *vice versa*. This pattern of $\Delta\rho^S$ shows that the spin projection causes a reduction of spin polarization in this system just like in the methyl and allyl radicals studied previously.[41]

Conclusion

The potential energy analysis shows great similarities for the monocation $[C(SH)_3]^+$ and its dication radical $[C(SH)_3]^{\bullet,2+}$. Open structures **1** and **2** are greatly favored. Cyclic distonic chiral stereoisomers **3b** do exist for the radical dication but—at least for the model systems discussed—they all are higher in energy. The C−S rotational barriers (**4** and **5**) and the high energies of the model structures **6** indicate strong π-interactions in **1** and **2**. Our best estimates for the rotational barriers of **1a** and **1b** are 9.2 and 3.3 kcal/mol, respectively, and the activation barriers for the least-energy automerizations of **2a** and **2b** are 8.5 and 4.7 kcal/mol. The radical dication C_{3h}-**1b** undergoes a Jahn−Teller deformation to form a modestly distorted structure **1b′** with one elongated and two shortened C−S bonds. The energy lowering due to the JT effect is only about 1 kcal/mol and pseudorotation in **1b** is essentially unhindered.

Dynamic electron correlation is important for the accurate calculation of the radical dication and the MO analysis shows why that is so. Removal of one electron from one of the degenerate π-HOMOs of **1a** results in a stabilization of the remaining π-electron to such an extent that *the unpaired electron is not in the HOMO of the dication*! Sets of spin-paired π- and σ-electrons both are higher in energy compared to the MO of the unpaired π-radical. Dynamic electron correlation is so important because of this readily identifiable feature of the molecular orbitals. The unpaired π-MO's "diving below the Fermi level" facilitates strong spin polarization because of energetic proximity with σ-MOs. The combination of annihilation of spin contamination and electron correlation is essential for the determination of relative energies.

Electron-deficient trivalent carbon intrinsically prefers trigonal-planar hybridization. It might be possible, however, to achieve pyramidalization of the trivalent carbon in heteroatom-substituted carbenium ions and our results suggest two strategies. All of the distonic ring structures **3b** are substantially pyramidalized at carbon. The pyramidalization might serve to reduce ring strain associated with the S−S interaction and, in effect, the pyramidalization reduces the distances between all three substituents. Hence, it might be possible to achieve C-pyramidalization by design of CX_3 systems that allow for stronger direct interactions between the X-substituents. Also, one could envision cations in which the C−S conformations of **6** are forced by embedding the system in a rigid framework.

Comparison of the hydride abstraction reactions of methane and its trithio derivative shows that the increased propensity for the formation of the trithio-substituted carbenium ion can be attributed to two substituent effects: A destabilization of the substituted methane and a stabilization of the cation formed. The latter effect is about twice as large compared to the former. At our highest level, we find that the computed hydride affinity of **1a** is about 95.5 kcal/mol less as compared to the respective experimental hydride affinity of methyl cation. The high magnitude of this value demonstrates in a compelling fashion the success of the basic approach of stabilizing carbenium ions by means of trithio substitution. The heat of formation of **1a**

was determined via the isodesmic reaction $CH_3^+ + 3CH_3SH \rightarrow 3CH_4 +$ **1a** and a value of ΔH_f(**1a**) = 197.7 kcal/mol resulted. The heat of formation ΔH_f(**1-H**) = 14.1 kcal/mol follows via the hydride abstraction reaction **1-H** $\rightarrow H^- +$ **1a**. With these enthalpies, the reduction of the heterolytic C−H bond dissociation energies of $HC(SH)_3$ compared to CH_4 was partitioned into a methane destabilization of 32.0 kcal/mol and a carbenium ion stabilization of 63.5 kcal/mol. Both effects must be considered in selections of R groups that might further facilitate the preparation of stabilized carbenium ions. Our best estimate for the ionization energy of **1a** is IP(**1a**) = 343.8 kcal/mol (14.9 eV) and results in ΔH_f(**1b**) = 541.5 kcal/mol.

The trithio-substituted cation and dication radical show the same electronic motif. While one might have expected to find charge dispersal due to S→C π-donation, a much larger S→C donation actually occurs in both the π- and σ-system. The result of the electron density shifts is a motif in which large positive charges are arranged around a *negative* carbon center. The oxidation of the monocation primarily removes sulfur π-electron density. The oxidation also removes some electron density from the central carbon and renders this C atom more π-acidic. The α-excess spin density is entirely concentrated on sulfur atoms and the carbon carries some β-spin density because of spin polarization. The results of the electronic structure analysis show that these S-containing carbenium ions are fundamentally different from the lighter O-homologs due to the *umpolung* of the C−X bonds. While the electronic structure of oxygen-stabilized carbenium ions is adequately described by the name, the trithio-substituted carbenium ions actually have methanide character associated with the central C atom and the name "sulfuronium ion" would not be inappropriate. Current theoretical and experimental studies are directed at exploring the chemistry suggested by the potential energy surface explorations and by the electronic structure analyses.

Acknowledgment. This research was supported by a NATO Collaborative Research Grant. R.G. thanks the donors of the Petroleum Research Fund, administered by the American Chemical Society, and the Research Board of the University of Missouri for additional support. We thank Steve Meyer of the MU Campus Computing Center for excellent systems services.

Supporting Information Available: Total energies and vibational zero-point energies of all structures (1 page). See any current masthead page for ordering and Internet access instructions.

JA960944H